

Real-Time Observation of Atomic Ordering in (001) $\text{In}_{0.53}\text{Ga}_{0.47}\text{As}$ Epitaxial Layers

B. A. Philips,^{1,*} I. Kamiya,^{2,†} K. Hingerl,^{2,‡} L. T. Florez,³ D. E. Aspnes,⁴ S. Mahajan,¹ and J. P. Harbison³

¹*Department of Materials Science and Engineering, Carnegie Mellon University, Pittsburgh, Pennsylvania 15213*

²*Department of Physics, University of Illinois, Urbana, Illinois 61801*

³*Bellcore, Red Bank, New Jersey 07701-7040*

⁴*Department of Physics, North Carolina State University, Raleigh, North Carolina 27695-8202*

(Received 4 November 1994)

We report the first real-time observation of atomic ordering in a semiconductor alloy during epitaxial growth. (001) $\text{In}_{0.53}\text{Ga}_{0.47}\text{As}$ layers deposited below about 400 °C exhibit a strong anisotropy in the *broadening parameters* of the $E_1, E_1 + \Delta_1$ transitions that is observable with reflectance-difference spectroscopy. This unusual optical behavior results from intraband mixing driven by triple-period ordering along both [111] and $[\bar{1}\bar{1}\bar{1}]$ directions simultaneously. This microstructure is realizable with stoichiometry $\text{In}_{0.556}\text{Ga}_{0.444}\text{As}$ virtually identical to that needed to lattice match InP.

PACS numbers: 68.55.Bd, 07.60.Fs, 71.25.Tn, 78.66.Fd

Since its initial observation in AlGaAs epitaxial layers grown on (110) GaAs substrates [1], atomic ordering has been found to occur in a variety of mixed III-V epitaxial materials [2–5]. The dominant form is of the type CuPt, where the periodicity along a $\langle 111 \rangle$ direction is doubled by a preferential occupancy of alternate $\{111\}$ planes by the two types of cations (or anions) [5]. Two triple-period variants were recently proposed by Gomyo *et al.* for $\text{Al}_{0.48}\text{In}_{0.52}\text{As}$, where threefold-periodic electron diffraction patterns were interpreted in terms of equal concentrations of domains with $\dots/\text{XYZ}/\text{XYZ}/\dots$ ordering along either the [111] or $[\bar{1}\bar{1}\bar{1}]$ directions [6]. Atomic ordering is of considerable technological interest because ordered layers exhibit smaller band gaps and higher carrier mobilities than their compositionally equivalent disordered analogs [2], and the prevailing surface reconstruction appears to play a major role [6–8].

Here, we report the first real-time observation of atomic ordering during epitaxial growth, specifically of (001) $\text{In}_{0.53}\text{Ga}_{0.47}\text{As}$ layers nominally lattice matched to InP. Our electron diffraction data also reveal triple periodicity, the first observed for this alloy. However, our optical data show that this arises from a *third* possibility, one where this periodicity occurs along the [111] and $[\bar{1}\bar{1}\bar{1}]$ directions *simultaneously* and not from a superpositioning of the [111] and $[\bar{1}\bar{1}\bar{1}]$ variants, a distinction that cannot be made from the electron diffraction patterns alone. Specifically, we find that $\text{In}_{0.53}\text{Ga}_{0.47}\text{As}$ grown below about 400 °C exhibits an anisotropy of 9 ± 2 meV of the *broadening parameter* of the E_1 and $E_1 + \Delta_1$ transitions, which is strong enough to be observable with reflectance-difference spectroscopy (RDS) during growth. This unusual optical behavior is found to result from simultaneous distortions of the otherwise nearly parallel bands along the [111] and $[\bar{1}\bar{1}\bar{1}]$ directions, leading us to this interpretation. A composition exhibiting the required periodicity has stoichiometry $\text{In}_{0.556}\text{Ga}_{0.444}\text{As}$ virtually identical to that needed to lattice match InP.

Experimental procedures were as follows. (001) InP substrates were prepared by standard chemical procedures and loaded into a Varian GEN-II molecular beam epitaxy (MBE) station. The native oxide was removed by heating to 540 °C in a flux of cracked As_4 . Nominally lattice-matched epitaxial layers of $\text{In}_{0.53 \pm 0.01}\text{Ga}_{0.47 \pm 0.01}\text{As}$ were deposited at 1 $\mu\text{m}/\text{h}$ at temperatures ranging from 350 to 500 °C with As_2 beam equivalent pressures (BEP) ranging from 0.6×10^{-6} to 3×10^{-6} Torr. Surface reconstructions were monitored by reflection high energy electron diffraction (RHEED). Optical anisotropies $\Delta r/r = \text{Re}(\Delta \tilde{r}/\tilde{r}) = 2 \text{Re}[(\tilde{r}_{\bar{1}10} - \tilde{r}_{110})/(\tilde{r}_{\bar{1}10} + \tilde{r}_{110})]$ were measured from 1.5 to 5.5 eV by RDS using methods and equipment described elsewhere [9]. The evolution of the anisotropy was also followed during epitaxy by kinetic RD measurements at a fixed energy of 2.5 eV. The microstructure of the ordered material was assessed by transmission electron microscopy.

RD spectra of optically thick atomically ordered and disordered layers are shown in Fig. 1. These data were taken during growth at 335 and 495 °C at BEPs of 0.6×10^{-6} and 2×10^{-6} , respectively. RHEED data obtained simultaneously showed weak (1×3) and (4×3) patterns, respectively. The RD spectrum of the disordered material is similar to that of the $c(4 \times 4)$ structure of (001) GaAs, i.e., characteristic of a surface terminated by two layers of As with the outer layer dimerized along the [110] direction. The ordered material exhibits additional structure near the E_1 , $E_1 + \Delta_1$, and E_2 critical points at about 2.40, 2.65, and 4.6 eV, respectively, at 335 °C. The E_1 and $E_1 + \Delta_1$ contributions have the same sign, thereby eliminating the linear electro-optic effect [10], or for that matter any electrooptic effect, as a possible mechanism.

Because above-band-gap optical anisotropies are almost always surface related, we first show that the additional anisotropy arises from the bulk. The relevant RD data, obtained kinetically at an energy of 2.5 eV, are given in Fig. 2. Here, an optically thick layer disordered material

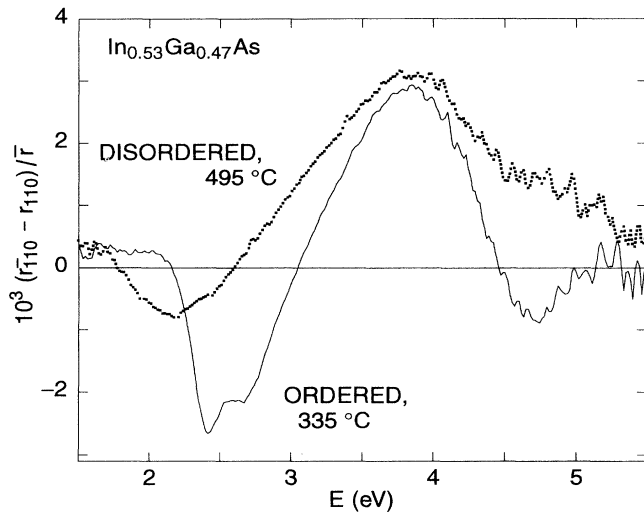


FIG. 1. RD spectra of atomically ordered (solid line) and disordered (points) $\text{In}_{0.53}\text{Ga}_{0.47}\text{As}$ obtained on optically thick films during epitaxial growth at the temperatures indicated.

was first deposited at 495 °C. The temperature was stabilized at 395 °C, a temperature at which ordering occurs, and a 1 min baseline was established. When growth was resumed the RD signal immediately began to rise and exhibited typical interference behavior as the thickness of the ordered layer increased. After the layer had become

optically thick, growth was again terminated and the temperature stabilized at 480 °C. When growth was resumed interference behavior was again observed. Because interference is more readily discernible in the complex $\Delta r/r$ plane, the inset of Fig. 2 shows the relationship between $\Delta r/r$ and $\Delta\theta$ as the thickness increases. The exponential-spiral behavior characteristic of interference is evident in both parts of the experiment. The small difference between initial and final points is due to a small difference in temperature.

The existence of these interference effects shows unequivocally that the dielectric properties of the materials deposited at 395 and 480 °C are different. Since the difference being measured is the optical anisotropy, it follows that the ordered material is optically anisotropic. With present sensitivity this ordering can be detected within the first 10 Å of growth.

The optical effects of ordering were also examined at room temperature, where reduced thermal broadening allowed the anisotropy to be examined in more detail. Figure 3 shows $\langle \epsilon_2 \rangle$ data for an ordered sample in the vicinity of the E_1 and $E_1 + \Delta_1$ transitions, where $\langle \epsilon \rangle = \langle \epsilon_1 \rangle + i\langle \epsilon_2 \rangle$ is the pseudo, or apparent, dielectric function measured by spectroellipsometry. The spectra were taken with the respective planes of incidence along the [110] and $[\bar{1}10]$ directions, the principal axes of the material. Since $\langle \epsilon \rangle$ is the projection of the dielectric tensor along the line formed by the intersection of the surface and the plane of incidence [11], these are the dielectric responses for light linearly polarized along the respective principal axes. The striking aspect is that the optical anisotropy is due primarily to an anisotropy in the *broadening parameter*, and not a dichroism of the E_1 and $E_1 + \Delta_1$ critical points. In particular, inspection of Fig. 3 shows that $\langle \epsilon_2 \rangle$ is substantially broader for light polarized along $[\bar{1}10]$ than for light polarized along [110]. This observation is supported by quantitative line shape analysis based on standard expressions where the contribution of a given critical point to $\langle \epsilon \rangle$ is represented as a function of energy E as $E - E_g + i\Gamma$, where E_g and Γ are the critical point energy and broadening parameter, respectively. We find that for $[\bar{1}10]$ polarization the broadening parameter is larger by 9 ± 2 meV, whereas the critical point thresholds are lower by 5 ± 1 meV.

Since lifetime affects broadening isotropically, the origin of this anisotropy must lie in the atomic ordering, which we now consider in detail. Figure 4(a) shows the electron diffraction pattern obtained in the $[\bar{1}10]$ section for the low-temperature material. The (000) spot is centered in the figure with (002), (111), $(11\bar{1})$, and $(00\bar{2})$ at the 12, 2, 4, and 6 o'clock positions, respectively. The superlattice streaks connecting (000) to (111) and $(11\bar{1})$ are prominent. Those associated with the higher-order spots clearly show the existence of a triple periodicity along the $[111]$ and/or the $[\bar{1}1\bar{1}]$ directions. In contrast, the [110] section shows only zinc-blende

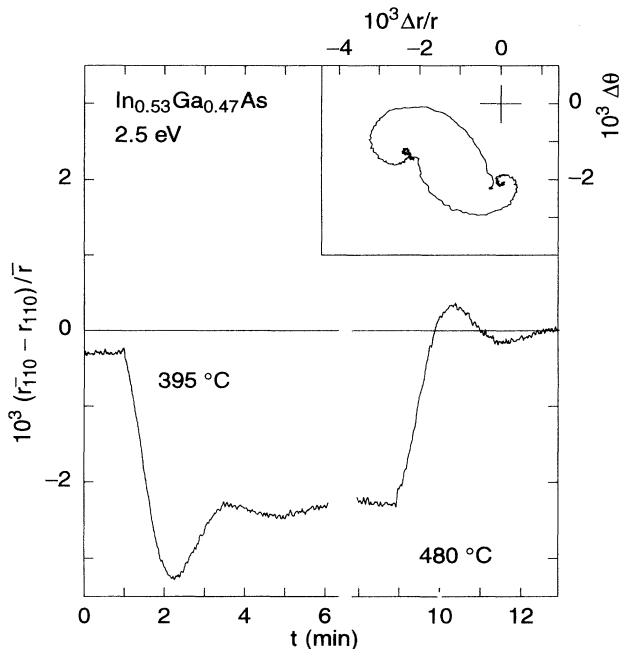


FIG. 2. RD transients at 2.5 eV for an atomically ordered layer growing on a disordered layer (left trace) and vice versa (right trace). The inset shows the $\Delta\theta$ vs $\Delta r/r$ trajectory of these transients.

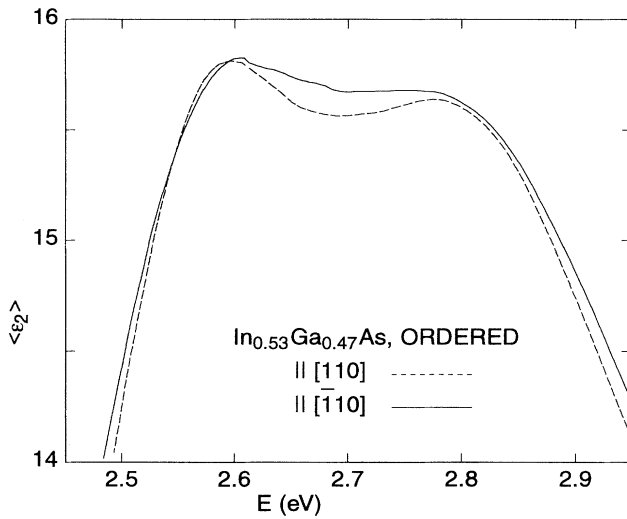


FIG. 3. Polarization dependence of the $\langle \epsilon_2 \rangle$ spectra of atomically ordered $\text{In}_{0.53}\text{Ga}_{0.47}\text{As}$ in the vicinity of the E_1 and $E_1 + \Delta_1$ transitions measured at room temperature.

features, indicating that triple periodicity does not occur along the $[\bar{1}11]$ and $[1\bar{1}\bar{1}]$ directions.

We now discuss the unusual optical behavior. Triple periodicity introduces terms $V_0 \cos(\mathbf{G}_1 \cdot \mathbf{r})$ and/or $V_0 \cos(\mathbf{G}_2 \cdot \mathbf{r})$ in the crystal potential, where \mathbf{G}_1 and \mathbf{G}_2 are $(2\pi/3a_0)(1, 1, 1)$ and $(2\pi/3a_0)(1, 1, \bar{1})$, respectively. Since the ordering is probably not perfect, we anticipate contributions from $(2\pi/3na_0)(1, 1, 1)$ and $(2\pi/3na_0)(1, 1, \bar{1})$ as well, where $n = 2, 3, \dots$. We consider first the valence and conduction bands along the $[111]$ direction, one of the four initially equivalent regions that give rise to the E_1 and $E_1 + \Delta_1$ structures. The periodic potential associated with \mathbf{G}_1 couples states separated by \mathbf{G}_1 . If the connected states have the same initial energy, an energy gap will be created. Since the intraband coupling strengths and energy dependences of the valence and conduction bands are different, the bands will be affected differently. These differences will broaden the formerly nearly constant interband energy along the $[111]$ and $[11\bar{1}]$ directions, leading to a corresponding broadening of the associated optical structure. In particular, the higher-order terms $(2\pi/3na_0)(1, 1, 1)$ and $(2\pi/3na_0)(1, 1, \bar{1})$ will be most effective near L , where the major contribution to E_1 and $E_1 + \Delta_1$ arises. In contrast, the $[\bar{1}11]$ and $[1\bar{1}\bar{1}]$ minima are not affected.

We now invoke the polarization selection rule, which states that the contribution of a $\langle 111 \rangle$ critical point is proportional to $1 - (\hat{\mathbf{k}} \cdot \hat{\mathbf{e}})^2$, where $\hat{\mathbf{k}}$ and $\hat{\mathbf{e}}$ are the unit direction and polarization vectors, respectively. For $\hat{\mathbf{e}} \parallel [\bar{1}10]$ the observed spectrum derives $\frac{3}{4}$ and $\frac{1}{4}$ of its oscillator strength from the coupled (broad) and uncoupled (sharp) bands, respectively. For $\hat{\mathbf{e}} \parallel [110]$ the figures are

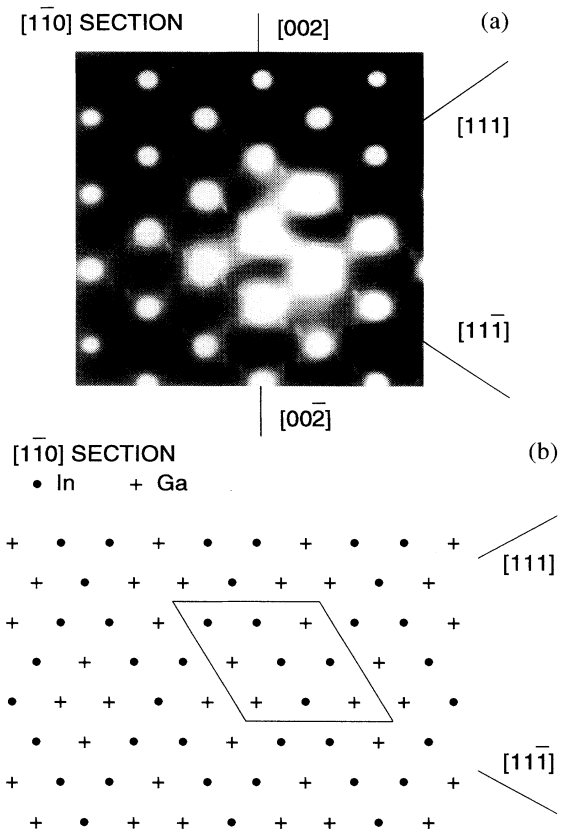


FIG. 4. (a) $[\bar{1}10]$ transmission electron micrograph of atomically ordered $\text{In}_{0.53}\text{Ga}_{0.47}\text{As}$. (b) Structural model with simultaneous triple periodicity along $[111]$ and $[11\bar{1}]$.

reversed. Thus $\langle \epsilon_2 \rangle$ should appear broader for $[\bar{1}10]$ polarization, as seen in Fig. 3. If the triple periodicity were limited to only one of the $\langle 111 \rangle$ directions the relative contributions would be $\frac{3}{8}$ and $\frac{5}{8}$ for $\hat{\mathbf{e}} \parallel [\bar{1}10]$ and $\frac{1}{8}$ and $\frac{7}{8}$ for $\hat{\mathbf{e}} \parallel [110]$. Although this smaller difference could still be detected by RDS, $\langle \epsilon_2 \rangle$ would be dominated by the unbroadened contribution for both polarizations, in contrast to the data. Thus triple periodicity must occur simultaneously along both $[111]$ and $[11\bar{1}]$ directions, resolving the electron diffraction “and/or” ambiguity in favor of “and.”

A composition exhibiting the required periodicity is shown in the $[\bar{1}10]$ section in Fig. 4(b), where the In and Ga species are represented by \bullet and $+$, respectively. The unit cell is necessarily 3×3 and contains nine atoms, five of which are In and four Ga. The associated stoichiometry is $\text{In}_{0.556}\text{Ga}_{0.444}\text{As}$, nearly identical to that required for lattice-matching InP.

More generally, for the more common CuPt periodicity band mixing will be limited to one direction in reciprocal space. As a result, the optical anisotropy and the strength of the associated RD signal will be reduced. For longer repeat periods of the “vertical superlattice” type \mathbf{G} is so short that the present mechanism will be effectively

suppressed, leading to optical spectra of the random-alloy type [12]. Thus a consistent picture is obtained. Detailed calculations will be presented elsewhere.

We are pleased to acknowledge support of this work by the Office of Naval Research under Contracts No. N-00014-90-J-1267 (I.K. and K.H.), No. N-00014-93-I-0255 (D.E.A.), and No. N-00014-92-J-1124 (B.A.P. and S.M.).

*Now at IBM Corporation, Essex Junction, VT 05452-4299.

†Now at IRC for Semiconductor Materials, Imperial College, London SW7 2BZ, UK.

‡Now at Lerchenring 11, A-4493 Wolfers, Austria.

- [1] T. S. Kuan, T. F. Kuech, W. I. Wang, and E. L. Wilkie, *Phys. Rev. Lett.* **54**, 201 (1985).
- [2] A. Gomyo, T. Suzuki, and S. Iijima, *Phys. Rev. Lett.* **60**, 2645 (1988); A. Chin, T. Y. Chang, A. Ourmazd, and E. M. Monberg, *Appl. Phys. Lett.* **58**, 968 (1991); D. J. Arent, M. Bode, K. A. Bertness, S. R. Kurtz, and J. M. Olson, *ibid.* **62**, 1806 (1993); T. Kanata, M. Nishimoto, H. Nakayama, and T. Nishino, *ibid.* **63**, 512 (1993).
- [3] S. R. Kurtz, J. M. Olson, and A. Kibbler, *Solar Cells* **24**, 307 (1988); *Appl. Phys. Lett.* **57**, 1922 (1990).
- [4] D. J. Mowbray, R. A. Hogg, M. S. Skolnick, M. C. DeLong, S. R. Kurtz, and J. M. Olson, *Phys. Rev. B* **46**, 7232 (1992); R. G. Alonso, A. Mascarenhas, G. S. Horner, K. A. Bertness, S. R. Kurtz, and J. M. Olson, *ibid.* **48**, 11 833 (1993).
- [5] A. Zunger and S. Mahajan, in *Handbook on Semiconductors*, edited by S. Mahajan (North-Holland, Amsterdam, 1994), Vol. 3, p. 1399.
- [6] A. Gomyo, K. Makita, I. Aono, and T. Suzuki, *Phys. Rev. Lett.* **72**, 673 (1994).
- [7] I. J. Murgatroyd, A. G. Norman, and G. R. Booker, *J. Appl. Phys.* **67**, 2310 (1990); S. Mahajan, in *Proceedings of the Fifth Brazilian School on Semiconductor Physics*, edited by J. R. Leite (World Scientific, Singapore, 1991), p. 79; S. Froyen and A. Zunger, *Phys. Rev. Lett.* **66**, 2132 (1991); T. Suzuki and A. Gomyo, *J. Cryst. Growth* **111**, 353 (1991); T. Suzuki and A. Gomyo, in *Physical Properties of Semiconductor Interfaces at Sub-Nanometer Scale*, edited by H. W. Salemink, NATO ASI Series (Kluwer, Dordrecht, 1994); L. C. Su, H. Ho, and G. B. Stringfellow, *Appl. Phys. Lett.* **65**, 749 (1994).
- [8] B. A. Philips, A. G. Noonan, T. Y. Tseong, S. Mahajan, G. R. Booker, M. Skowronski, J. P. Harbison, and V. G. Keramidas, *J. Cryst. Growth* **140**, 249 (1994); B. A. Philips, R. McFadden, J. P. Harbison, M. Tanaka, and S. Mahajan, *Mater. Sci. Engineering B* (to be published).
- [9] D. E. Aspnes, J. P. Harbison, A. A. Studna, and L. Florez, *J. Vac. Sci. Technol. A* **6**, 1327 (1988).
- [10] S. Acosta-Ortiz and A. Lastras-Martinez, *Solid State Commun.* **64**, 809 (1987).
- [11] D. E. Aspnes, *J. Opt. Soc. Am.* **70**, 1275 (1980).
- [12] H. Kanbe, A. Chavez-Pirson, H. Ando, H. Saito, and T. Fukui, *Appl. Phys. Lett.* **58**, 2969 (1991).

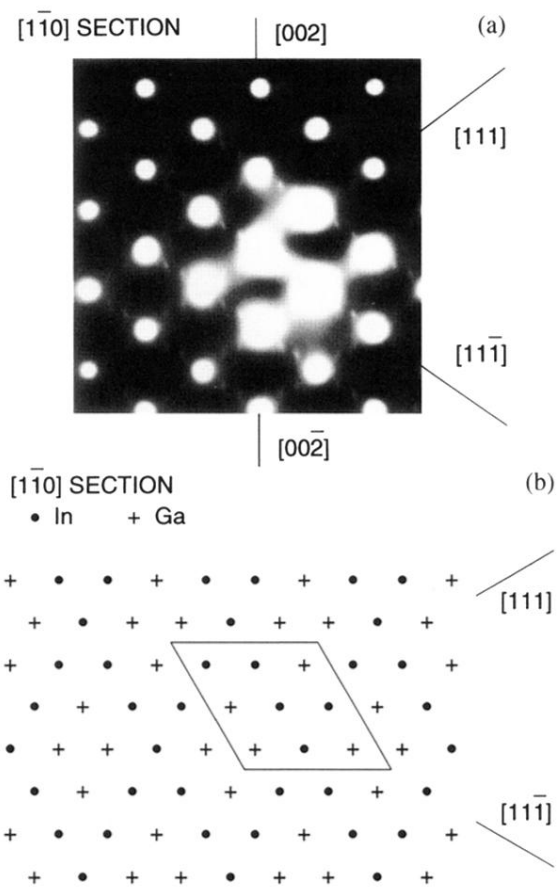


FIG. 4. (a) $[1\bar{1}0]$ transmission electron micrograph of atomically ordered $\text{In}_{0.53}\text{Ga}_{0.47}\text{As}$. (b) Structural model with simultaneous triple periodicity along $[111]$ and $[1\bar{1}\bar{1}]$.